Quantification of Ultrasonic Motor Behaviour in MRI

Peyman Shokrollahi[1], Wendong Wang[2], Adam C. Waspe[3], James M. Drake[3], and Andrew A. Goldenberg[1]

[1]*Institute of Biomaterials and Biomedical Engineering, University of Toronto, Toronto, ON, Canada,* [2]*School of Mechanical Engineering, Northwestern Polytechnical University, Xi'an, Shaanxi, China,* [3]*Hospital for Sick Children, Toronto, ON, Canada*

Target Audience

The target audience includes researchers, engineers and clinicians who are interested in tele-surgery, MRI-compatible devices, and bone biopsy procedures.

Purpose

Obtaining haptic information and controlling the force produced by actuators is one of the key issues in performing a successful operation by surgical robots. However, force and kinesthetic information are still not fully available to the surgeon in an MR environment [1]. In addition, the behaviour of actuators such as ultrasonic motors (USMs) in an MR environment is unknown and needs to be characterized. The characteristic quantification of the actuators in MR environment can additionally be used to optimize motor performance, develop the actuators for haptic devices, and designing MRI-compatible diagnostic and therapeutic tools for real-time applications. The advantages of USMs (small size and large torque) are significant for the design of MRI-compatible surgical tools where large forces are required, such as skull drilling in neurosurgery or bone biopsies. Although USMs are MR-safe actuators with little to no effect on image quality when they are located at specific distances from the bore centre, their physical characteristics (e.g. torque, speed, and position) in the MR environment are still unknown [2, 3]. Quantifying the device characteristics is also not possible due to the compatibility limitations of available measuring tools. To perform pediatric bone penetration procedures in MRI, we are developing an MRI-compatible surgical robot utilizing USMs actuators and quantifying the motor's axial force, with an MRI-compatible force feedback system.

Methods

A one DoF robot (Fig. 1) was built from MR-compatible materials (Ultem, Delrin, and high-density polyethylene) to measure the torque produced by the USM motor (PUMR40, PiezoElectric Technology Co., Ltd., South Korea) and transferred as an axial force by using a screw. The axial force was measured with a piezo-resistive sensor (Tekscan Flexiforce sensor, A201). The robot was placed near the isocentre in a 3T Achieva scanner (Philips Healthcare, Best, NL). The magnitude and phase images were acquired utilizing three sequences: FFE, b-FFE, and TSE (TE = 72 ms, TR = 4.0 s, FOV = 200 mm, in-plane voxel size = 1.5 mm, slice thickness = 5 mm (Fig. 2))[4]. A mineral oil phantom (Phillips) was placed at the side of the robot adjacent to the motor and sensor's system to acquire the transverse and coronal images. The robot controllers and acquisition systems were located in the control room and the cables were shielded. The axial applied force was generated by driving the phantom needle mounted on top of the sensor, both inside and outside the MR environment. The acquired data was processed for further analysis using MATLAB 2013b.

Results and Discussions

The end effector of the robot (needle) was cycled periodically at 3.0 s intervals. The axial force was measured with (load) and without (no-load) contact to a barrier by a calibrated output voltage of the sensor, outside and inside the MRI for both forward and reverse directions (Table 1) [5]. There were inertial forces in the no-load state. The measured force values were the same for all three imaging sequences. Although the backward force was smaller than the forward one out of MRI, it was larger than the forward one in the MRI (Fig. 3). In the load state, the forces inside MRI are almost two times as large as those measured outside MRI, and similarly the backward motion produces larger force than the forward one inside MRI, with the opposite effect outside MRI (Fig. 3).

Table 1 Statistical Analysis of forces (N) is side and outside MRI at no-load and with load states

No Load	Outside MRI								Inside MRI							
	Forward				Backward				Forward				Backward			
	Mean (N)		STD		Mean (N)		STD		Mean (N)		STD		Mean (N)		STD	
	21		0.008		20		0.005		61		0.005		69		0.005	
With Load	Inside MRI								Outside MRI							
	Forward				Backward				Forward				Backward			
	Min (N)		Max (N)		Min (N)		Max (N)		Min (N)		Max (N)		Min (N)		Max (N)	
	Mean	STD	Mean	STD	Mean	STD	Mean	STD	Mean	STD	Mean	STD	Mean	STD	Mean	STD
	20	0	33	0.01	20	0	31	0.02	61	0.01	81	0.08	68	0.01	80	0.02

Conclusion

The USM characteristics are different inside and outside the MRI. The backward motion produced a larger force than the forward one inside the MRI and this behaviour was opposite outside MR environment. Also, the measured force was almost doubled while the motor was running during the MR scan. The reason of this change is due to effects of magnetic field on the motor's behaviour. The nonlinearity in the motor behaviour should be modeled precisely to harness the force inside MR environment. Quantifying the effects of MRI on the motor characteristics can be used for the better control of actuators and developing an MRI-compatible haptic device.

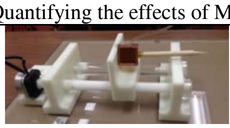

Fig.1 MRI-compatible robot.

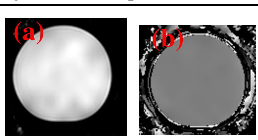

Fig. 2 TSE transverse image of the phantom.

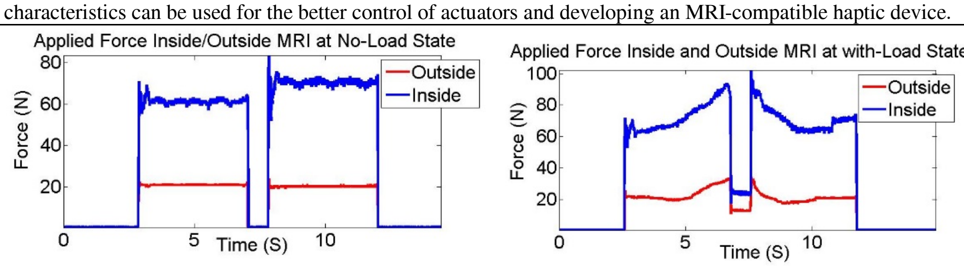

Fig. 3 Applied force at no-load and with-load states.

[1] Puangmali P, *et al,* "State-of-the-Art in Force and Tactile Sensing for Minimally Invasive Surgery," IEEE Sensors Journal, **8**(4):371–381 (2008).

[2] Chinzei K, *et al,* "MR compatibility of mechatronic devices: design criteria," MICCAI, 1020—1030 (1999).

[3] Elhawary H, *et al*, "A review of magnetic resonance imaging compatible manipulators in surgery," PI MECH ENG H, 3(220):413-424 (2005).

[4] Wang W, *et al*, "Compatibility of US motors for development of MRI-guided surgical robot," IEEE, Biomedical Eng & Informatics (2013).

[5] Armitage P, *et al,* "Statistical methods in medical research," John Wiley & Sons, 137-146 (2008).